Available online at www.sciencedirect.com
ScienceDirect
Journal of Sound and Vibration 306 (2007) 318–332
JOURNAL OF SOUND AND VIBRATION
www.elsevier.com/locate/jsvi

Piezoelectric generation of extensional waves in a viscoelastic bar by use of a linear power amplifier: Theoretical basis

A. Jansson*, B. Lundberg

The Ångström Laboratory, Uppsala University, Box 534, SE-751 21 Uppsala, Sweden

Received 14 July 2006; received in revised form 2 May 2007; accepted 3 May 2007
Available online 27 June 2007

Abstract

A system consisting of a linear power amplifier driving a piezoelectric actuator pair attached to a long viscoelastic bar is analysed. Coupled piezoelectric theory is used, and allowance is made for the dynamics of the amplifier and of the actuators. Formulae are derived for the relation between the input voltage to the amplifier and the normal force associated with extensional waves generated in the bar and for the load impedance constituted by the actuator-bar assembly. It is established that the mechanical work performed on the external parts of the bar at the actuator/bar interfaces is at most equal to the electrical energy supplied by the amplifier. The results are applied to a three-parameter viscoelastic bar and to an elastic bar, and the effects of the cut-off frequency, without load, and the output impedance of the amplifier are examined. For the elastic bar, sharp response minima occur at frequencies that are integral multiples of the inverse transit time through the actuator region. For the viscoelastic bar, the corresponding minima are less sharp and deep. The input voltage to the amplifier required to produce a desired output wave at the actuator/bar interfaces can be determined provided that the spectrum of this wave is not too broad.

1. Introduction

Piezoelectric elements in the form of thin plates are increasingly used as sensors, e.g. Refs. [1,2], and actuators, e.g. Refs. [3,4], in structural, space, medical and other applications. Their fundamentally important feature in this context is that they give electrical response when subjected to mechanical stimuli, and vice versa. This dual property is described by two coupled constitutive equations [5], often referred to as the actuator equation and the sensor equation, that relate the mechanical and electrical fields in the piezoelectric material. Such piezoelectric elements have large bandwidth and are suitable for integration into structures.

An analysis of the interaction of a piezoelectric actuator, driven by a linear power amplifier, and a host structure generally involves consideration of the two constitutive equations, the dynamics of the amplifier and associated electric circuits, the dynamics of the actuator, and the dynamics of the host structure. Under special circumstances, one or several of these considerations may be insignificant.

*Corresponding author.
E-mail address: anders.jansson@angstrom.uu.se (A. Jansson).

0022-460X/$ - see front matter © 2007 Elsevier Ltd. All rights reserved.
doi:10.1016/j.jsv.2007.05.005

Nomenclature

A	cross-sectional area
c	wave speed
C	capacitance
d	piezoelectric constant
D	electric displacement
e	strain
E	complex modulus, Young's modulus
f	frequency
F	frequency-dependent part of transfer function H
G	voltage gain of amplifier
h	height
H	transfer function, voltage to normal force
i	current
k	square root of piezoelectric coupling coefficient
l	length
N	normal force
Q	charge
R	resistance
t	time
U	voltage
v	particle velocity
w	width
W	energy, work
x	axial coordinate
y	transverse coordinate (horizontal)
z	transverse coordinate (vertical)
Z	impedance, characteristic impedance

Greek

γ	wave propagation coefficient
ε	permittivity
ζ	impedance ratio
ρ	density
ω	angular frequency

Superscripts

0	ideal amplifier
av	spatial average
c	creep
e	elastic
emf	electromotive force
E	electrical
M	mechanical
r	relaxation

Subscripts

0	actuator region
a	actuator
b	bond
c	core
cut	cut-off (3 dB reduction)
L	loaded amplifier
n	propagation in direction of decreasing x
out	amplifier output
p	propagation in direction of increasing x
ref	reference value

The sensor equation and the dynamics of the amplifier can be neglected if the actuator is driven directly from an amplifier with sufficiently low-output impedance and of sufficiently large bandwidth. Furthermore, the actuator may be considered as quasi-static if it is sufficiently small. Such simplifications were made in the early work by Crawly and de Luis [6] on the interaction of piezoelectric actuators and an Euler–Bernoulli beam.

The dynamics of the actuator was taken into account, e.g., by Pan et al. [7], who studied an Euler–Bernoulli beam with attached piezoelectric actuators. Allowance for the interaction of structure and electrical circuits, and for the two coupled constitutive equations, was made, e.g., by Hagood et al. [8], Thornburgh and Chattopadhyay [9], and Thornburgh et al. [10]. Similar considerations were made also in studies of passive electrical damping systems [11]. Studies of power requirements, with consideration of the dynamics of the amplifier, were carried out, e.g., by Niezrecki and Cudney [12] and Leo [13].

In control applications involving waves, a problem of fundamental interest is that of generating waves of prescribed shapes that can be used to cancel disturbing waves. Yet, little related work seems to have been done. In particular, no such work has been found that involves viscoelastic structures or structural members. Therefore, the problem to be considered in this paper is that of generating extensional waves in a linearly viscoelastic bar by means of a linear power amplifier driving an in-phase symmetric piezoelectric actuator pair. As a special case, the bar may be linearly elastic.

Both the problem of finding the wave output produced by a given voltage input to the amplifier and the converse problem of finding the voltage input to the amplifier required to generate a desired wave output will be considered. The consistency of the model used will be confirmed by establishing that the mechanical work performed by the actuators on the external parts of the bar is at most equal to the electrical energy supplied by the amplifier. An associated problem to be considered is that of determining the electrical impedance that constitutes the load of the amplifier.

In Section 2, the interaction of amplifier, actuators and bar will be studied for a general linear amplifier and for a general linearly viscoelastic material. Coupled piezoelectric theory will be used, and full allowance will be made for the dynamics of the amplifier. The dynamics of the actuators and the bar will be taken into account in a one-dimensional context. In Section 3, the theoretical results obtained will be applied to a specific amplifier model and to a three-parameter viscoelastic material as well as to a linearly elastic material. Numerical results will be presented and discussed together with other results in Section 4, and conclusions will be stated in Section 5.

2. Theory

2.1. Model description

Consider a long viscoelastic bar with an attached symmetrical pair of piezoelectric actuators of length $l_0 = 2x_0$ in the actuator region $-x_0 < x < x_0$, where x is an axial coordinate as shown in Fig. 1. The actuators are attached to the bar by bonding layers of finite thickness. The cross-sections of the bar, the actuators and the bonding layers are rectangular, and the full cross-sections are symmetric with respect to the y and z axes.

Outside the actuator region, the bar has height h, width w and cross-sectional area $A = hw$. In the core of the actuator region, it has height h_c, width w_c and cross-sectional area $A_c = h_c w_c$. Each bonding layer has height h_b, width w_b and cross-sectional area $A_b = h_b w_b$, and each actuator has height h_a, width w_a and cross-sectional area $A_a = h_a w_a$. Therefore, within the actuator region, the total cross-sectional area is $A_0 = 2A_a + 2A_b + A_c$.

Generally, the materials of the bar and the bonding layers are assumed to be viscoelastic with complex moduli $E(\omega)$, $E_b(\omega)$, respectively, where ω is the angular frequency, while the material of the actuators is assumed to be elastic with short-circuited Young's modulus E_a. As important special cases, one or both of the materials of the bar and the bonding layers may be considered elastic by taking the moduli E and/or E_b as real-valued and constant. This is the normal choice of E, e.g., if the bar is metallic.

It is further assumed that initially plane cross-sections remain plane and that the stress is uniaxial in the x direction. Within the actuator region, therefore, the effective complex modulus is $E_0 = (2A_aE_a + 2A_bE_b + A_cE)/A_0$. Similarly, the effective density within this region is $\rho_0 = (2A_a\rho_a + 2A_b\rho_b + A_c\rho)/A_0$, where ρ, ρ_b and ρ_a are the densities of the materials of the bar, the bonding layers and the actuators, respectively.

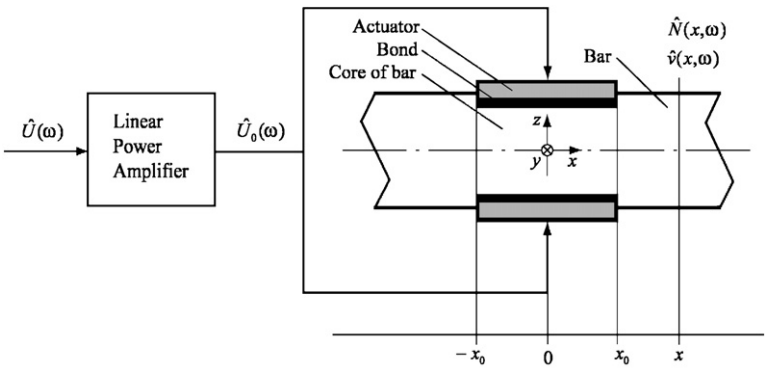

Fig. 1. Linear power amplifier, actuators and bar.

The piezoelectric material is assumed to be polarized in the z direction and to have a linear electromechanical response. In addition to the short-circuited Young's modulus E_a, this response is characterised by the permittivity ε_a and the piezoelectric constant $d_a = -d_{31}$. The electrical fields between the conducting layers on the upper and lower faces of the actuators are assumed to be parallel to the z-axis. The electric displacement field is assumed to depend on x and ω, while the electric field strength is assumed to depend on ω only. The effects of strains in the y and z directions are neglected.

The actuators are driven in parallel and in phase by the output voltage and current of a linear power amplifier. The amplifier is characterised by its voltage gain $G(\omega)$, when unloaded, and its output impedance $Z^E_{\text{out}}(\omega)$. As a result of the mechanical response of the actuators, extensional waves are generated which propagate symmetrically in opposite directions through the bar away from the actuator region.

2.2. Amplifier and actuators

The amplifier, represented by its assumed equivalent circuit, and the two piezoelectric actuators in parallel are shown in Fig. 2. The output voltage $\hat{U}_0(\omega)$ is related to the input voltage $\hat{U}(\omega)$ and the output current $\hat{i}_0(\omega)$ by the relation

$$\hat{U}_0 = G\hat{U} - Z^E_{\text{out}}\hat{i}_0. \tag{1}$$

Here and in what follows, the notation $\hat{\Phi}(\omega)$ is used for the Fourier transform of a function $\Phi(t)$, which is assumed to be piecewise differentiable and absolutely integrable.

Under the conditions assumed, the coupled constitutive equations [5] of the piezoelectric material can be written

$$\hat{e} = \frac{1}{E_a}\frac{\hat{N}_a}{A_a} - d_a\frac{\hat{U}_0}{h_a}, \tag{2}$$

$$\hat{D}_a = -d_a\frac{\hat{N}_a}{A_a} + \varepsilon_a\frac{\hat{U}_0}{h_a}, \tag{3}$$

where $\hat{e}(x,\omega)$ is the normal strain and $\hat{N}_a(x,\omega)$ the normal force in the x direction, $\hat{D}_a(x,\omega)$ the electric displacement and $\hat{U}_0(\omega)$ the voltage across the actuators in the z direction.

In terms of the electric displacement field, the charge on each actuator becomes

$$\hat{Q}_a(\omega) = \int_{-x_0}^{x_0} \hat{D}_a(x,\omega) w_a \,\mathrm{d}x. \tag{4}$$

The output current from the amplifier to the two actuators in parallel is related to this charge through

$$\hat{i}_0 = 2\mathrm{i}\omega\hat{Q}_a, \tag{5}$$

where i is the imaginary unit. By the use of Eqs. (3) and (4), this relation can be turned into the form

$$\hat{i}_0 = \frac{1}{Z^E_0}\left(\hat{U}_0 - \hat{U}^{\text{emf}}_a\right), \quad \hat{U}^{\text{emf}}_a = \frac{d_a h_a}{\varepsilon_a A_a}\hat{N}^{\text{av}}_a, \tag{6a,b}$$

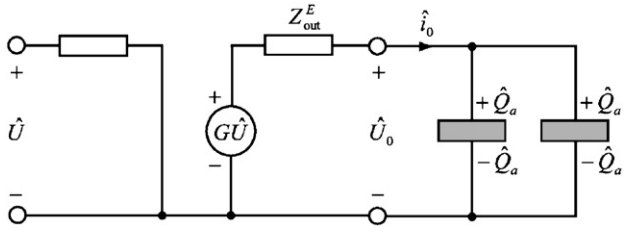

Fig. 2. Equivalent circuit of linear power amplifier driving piezoelectric actuator pair.

where $Z_0^E = Z_a^E/2$ with $Z_a^E(\omega) = 1/\mathrm{i}\omega C_a$ and $C_a = \varepsilon_a l_0 w_a/h_a$. Here, $\hat{U}_a^{\mathrm{emf}}$ is an electromotive force directly proportional to the spatial average $\hat{N}_a^{\mathrm{av}}(\omega) = (1/l_0)\int_{-x_0}^{x_0} \hat{N}_a(x,\omega)\,\mathrm{d}x$ of the normal force $\hat{N}_a(x,\omega)$ in each actuator. Thus, C_a can be interpreted as the capacitance of an unloaded actuator, $Z_a^E(\omega)$ as the corresponding electrical impedance, and Z_0^E as the electrical impedance of two such actuators in parallel.

By Eqs. (1), (2) and (6), the normal force $\hat{N}_a(x,\omega)$ in each actuator is related to the strain $\hat{e}(x,\omega)$ and the input voltage $\hat{U}(\omega)$ to the amplifier by the integral equation

$$\hat{N}_a - \frac{\zeta}{1+\zeta}k^2\hat{N}_a^{\mathrm{av}} = A_a E_a \hat{e} + A_a E_a \frac{d_a}{h_a}\frac{1}{1+\zeta}G\hat{U}, \tag{7}$$

where

$$\zeta = \frac{Z_{\mathrm{out}}^E}{Z_0^E}, \quad k^2 = \frac{d_a^2 E_a}{\varepsilon_a} \tag{8a,b}$$

are the amplifier output to unloaded actuator pair electrical impedance ratio and the piezoelectric coupling coefficient [5], respectively.

2.3. Actuators and bar

In the actuator region $-x_0 < x < x_0$, the equation of motion

$$\frac{\partial \hat{N}}{\partial x} = \rho_0 A_0 \mathrm{i}\omega\hat{v} \tag{9}$$

and the condition of compatibility

$$\hat{e} = \frac{1}{\mathrm{i}\omega}\frac{\partial \hat{v}}{\partial x} \tag{10}$$

relate the normal force

$$\hat{N} = 2\hat{N}_a + 2\hat{N}_b + \hat{N}_c, \tag{11}$$

the particle velocity $\hat{v}(x,\omega)$ and the strain $\hat{e}(x,\omega)$. The contribution to the normal force $\hat{N}(x,\omega)$ from each actuator $\hat{N}_a(x,\omega)$ is given by Eq. (7), while those from each bonding layer $\hat{N}_b(x,\omega)$ and the bar $\hat{N}_c(x,\omega)$ are given by the constitutive relationships

$$\hat{N}_b = A_b E_b \hat{e}, \quad \hat{N}_c = A_c E \hat{e}. \tag{12a,b}$$

Because of symmetry, $\hat{N}(x,\omega)$ and $\hat{v}(x,\omega)$ are even and odd functions, respectively, of x.

Eqs. (7) and (9)–(12) provide one integral equation, two differential equations and three algebraic equations for the six unknown functions $\hat{N}(x,\omega)$, $\hat{N}_a(x,\omega)$, $\hat{N}_b(x,\omega)$, $\hat{N}_c(x,\omega)$, $\hat{v}(x,\omega)$ and $\hat{e}(x,\omega)$ in the actuator region. Therefore, the general solution for $\hat{N}(x,\omega)$ and $\hat{v}(x,\omega)$ can be derived from these equations. By Eqs. (7) and (10)–(12), the normal force can be expressed as

$$\hat{N} = A_0 E_0 \frac{1}{\mathrm{i}\omega}\frac{\partial \hat{v}}{\partial x} + \frac{2\zeta}{1+\zeta}k^2\hat{N}_a^{\mathrm{av}} + 2A_a E_a \frac{d_a}{h_a}\frac{G\hat{U}}{1+\zeta}. \tag{13}$$

Here, the average normal force $\hat{N}_a^{\mathrm{av}}$ is obtained by substituting Eq. (10) into Eq. (7) and forming the spatial average of each term. This gives

$$\hat{N}_a^{\mathrm{av}} = \frac{1+\zeta}{1+\zeta(1-k^2)}Z_a^M[\hat{v}(x_0,\omega) - \hat{v}(-x_0,\omega)] + A_a E_a \frac{d_a}{h_a}\frac{G\hat{U}}{1+\zeta(1-k^2)}, \tag{14}$$

where $Z_a^M = A_a E_a/\mathrm{i}\omega l_0$. Substitution of this result into Eq. (13) gives the normal force in the actuator region

$$\hat{N} = A_0 E_0 \frac{1}{\mathrm{i}\omega}\frac{\partial \hat{v}}{\partial x} + \frac{2\zeta k^2}{1+\zeta(1-k^2)}Z_a^M[\hat{v}(x_0,\omega) - \hat{v}(-x_0,\omega)] + 2A_a E_a \frac{d_a}{h_a}\frac{G\hat{U}}{1+\zeta(1-k^2)}, \tag{15}$$

which, when substituted into the equation of motion (9), gives the Fourier transformed wave equation

$$\frac{\partial^2 \hat{v}}{\partial x^2} - \gamma_0^2 \hat{v} = 0 \tag{16}$$

in terms of particle velocity.

The most general solution of Eqs. (15) and (16), which satisfies the symmetry requirements $\hat{N}(-x,\omega) = \hat{N}(x,\omega)$ and $\hat{v}(-x,\omega) = -\hat{v}(x,\omega)$ can be expressed as

$$\hat{N} = \hat{N}_{0p}\left[e^{-\gamma_0 x} + e^{\gamma_0 x} + \frac{4\zeta k^2}{1+\zeta(1-k^2)}\frac{Z_a^M}{Z_0^M}(-e^{-\gamma_0 x_0} + e^{\gamma_0 x_0})\right] + 2A_a E_a \frac{d_a}{h_a}\frac{G\hat{U}}{1+\zeta(1-k^2)}, \tag{17}$$

$$\hat{v} = \frac{\hat{N}_{0p}}{Z_0^M}(-e^{-\gamma_0 x} + e^{\gamma_0 x}), \tag{18}$$

where $\gamma_0 = \mathrm{i}\omega/c_0$ is the wave propagation coefficient and $Z_0^M = A_0 E_0/c_0$, with $c_0 = (E_0/\rho_0)^{1/2}$, is the characteristic impedance in the actuator region. The function $\hat{N}_{0p}(\omega) = \hat{N}_{0n}(\omega)$ is arbitrary and represents the normal force amplitudes at $x = 0$ of waves $\hat{N}_{0p}e^{-\gamma_0 x}$ and $\hat{N}_{0n}e^{\gamma_0 x}$ travelling within the actuator region $-x_0 < x < x_0$ in the directions of increasing and decreasing x, respectively.

In the bar region $x \geqslant x_0$, where waves are travelling only in the direction of increasing x, the general solution

$$\hat{N} = \hat{N}_p e^{-\gamma(x-x_0)}, \tag{19}$$

$$\hat{v} = -\frac{1}{Z^M}\hat{N}_p e^{-\gamma(x-x_0)} \tag{20}$$

for the normal force $\hat{N}(x,\omega)$ and the particle velocity $\hat{v}(x,\omega)$ can be obtained by reinterpreting the first terms of Eqs. (17) and (18). Here, $\gamma = \mathrm{i}\omega/c$ is the wave propagation coefficient and $Z^M = AE/c$, with $c = (E/\rho)^{1/2}$, is the characteristic impedance of the bar. The function $\hat{N}_p(\omega)$ is arbitrary and represents the normal force amplitude at $x = x_0$ of a wave $\hat{N}_p e^{-\gamma(x-x_0)}$ travelling in the bar region $x \geqslant x_0$ in the direction of increasing x.

The two functions $\hat{N}_{0p}$ and $\hat{N}_p$, representing the waves in the actuator and bar regions, can be determined by the conditions of continuity of normal force $\hat{N}(x_0-,\omega) = \hat{N}(x_0+,\omega)$ and particle velocity $\hat{v}(x_0-,\omega) = \hat{v}(x_0+,\omega)$ at $x = x_0$. Substituting Eqs. (17)–(20) into these conditions and solving for $\hat{N}_p$ gives

$$\hat{N}_p = HG\hat{U}, \tag{21}$$

where

$$H = 2A_a E_a \frac{d_a}{h_a}F, \quad F = \frac{e^{\gamma_0 x_0} - e^{-\gamma_0 x_0}}{pe^{\gamma_0 x_0} - qe^{-\gamma_0 x_0}}, \tag{22a,b}$$

$$p = \left(1 + \frac{Z_0^M}{Z^M}\right)\left[1 + (1-k^2)\frac{Z_{\mathrm{out}}^E}{Z_0^E}\right] + 4k^2\frac{Z_a^M}{Z^M}\frac{Z_{\mathrm{out}}^E}{Z_0^E}, \tag{22c}$$

$$q = \left(1 - \frac{Z_0^M}{Z^M}\right)\left[1 + (1-k^2)\frac{Z_{\mathrm{out}}^E}{Z_0^E}\right] + 4k^2\frac{Z_a^M}{Z^M}\frac{Z_{\mathrm{out}}^E}{Z_0^E}. \tag{22d}$$

Substitution of Eq. (21) into Eq. (19) gives the normal force in the bar at $x \geqslant x_0$

$$\hat{N} = HG\hat{U}e^{-\gamma(x-x_0)} \tag{23}$$

in terms of the input voltage to the amplifier.

2.4. Energy considerations

The process of wave generation in the two external parts of the bar involves partial conversion of the electrical energy

$$W^E = \int_{-\infty}^{\infty} U_0(t) i_0(t)\,\mathrm{d}t = \frac{1}{2\pi}\int_{-\infty}^{\infty} \overline{\hat{U}_0(\omega)}\hat{i}_0(\omega)\,\mathrm{d}\omega \tag{24}$$

supplied to the actuators into the mechanical work

$$W^M = -2\int_{-\infty}^{\infty} N_0(t)v_0(t)\,\mathrm{d}t = -\frac{1}{\pi}\int_{-\infty}^{\infty} \overline{\hat{N}_0(\omega)}\hat{v}_0(\omega)\,\mathrm{d}\omega \tag{25}$$

performed by the actuators on the external parts of the bar at the actuator/bar interfaces $x = \pm x_0$, where the notation $\bar{\Phi}$ is used for the complex conjugate of Φ. In the last members of these relations, use has been made of Parseval's relation. The minus sign in the last relation is due to the different positive directions of the normal force $N_0(t) = N(x_0, t)$ and the particle velocity $v_0(t) = v(x_0, t)$.

The electric impedance Z^E loading the amplifier is defined by the relation

$$\hat{U}_0 = Z^E\hat{i}_0. \tag{26}$$

A convenient way to derive this impedance from results obtained makes use of its independence of the output impedance of the amplifier, which can therefore be taken as zero. Thus, Eqs. (1), (6), (8), (14), (20), (21) with $Z^E_{\mathrm{out}} = 0$, and symmetry considerations, give

$$Z^E = \frac{Z^E_0}{1 - k^2(1 - 4F^0 Z^M_a/Z^M)}, \tag{27}$$

where $F^0(\omega)$ is obtained from $F(\omega)$ by putting $Z^E_{\mathrm{out}} = 0$ in Eqs. (22b)–(22d). Substitution of $\hat{i}_0$ from Eq. (26) into Eq. (24) gives

$$W^E = \frac{1}{2\pi}\int_{-\infty}^{\infty} \frac{1}{Z^E}\left|\hat{U}_0\right|^2 \mathrm{d}\omega. \tag{28}$$

By Eqs. (19) and (20), the normal force $\hat{N}_0(\omega)$ and the particle velocity $\hat{v}_0(\omega)$ produced at the actuator/bar interface $x = x_0$ are related as

$$\hat{N}_0 = -Z^M\hat{v}_0. \tag{29}$$

Substitution of $\hat{v}_0$ from Eq. (29) into (25) gives

$$W^M = \frac{1}{\pi}\int_{-\infty}^{\infty} \frac{1}{Z^M}\left|\hat{N}_0\right|^2 \mathrm{d}\omega. \tag{30}$$

From Eqs. (28) and (30) and results of Sections 2.1–2.3, and by use of the result obtained by Christensen [14] that the complex modulus is located in the first quadrant of the complex plane for $\omega > 0$, it can be shown that

$$0 < W^M \leqslant W^E \tag{31}$$

with equality if and only if the effective complex modulus E_0 in the actuator region is real.

3. Applications

It will be illustrated how the relation between the normal force $N(x, t)$ in the bar and the input voltage to the amplifier $U(t)$ depends on the cut-off frequency $\omega_{\mathrm{cut}} = 2\pi f_{\mathrm{cut}}$ and the output impedance Z^E_{out} of the amplifier. In the frequency domain, these dependencies are related to the voltage gain $G(\omega)$ and the function $H(\omega)$, respectively. The dependence on frequency $\omega = 2\pi f$ of the electrical impedance $Z^E(\omega)$, which constitutes the load of the amplifier, will also be illustrated.

An amplifier with voltage gain

$$G = \frac{G^0}{1 + \mathrm{i}\omega/\omega_{\mathrm{cut}}} \tag{32}$$

is considered. Here, $\omega_{\mathrm{cut}} = 2\pi f_{\mathrm{cut}}$ is the cut-off angular frequency at which $|G(\omega)|$ is 3 dB below its real low-frequency limit G^0, i.e., $|G(\omega_{\mathrm{cut}})| = G^0/\sqrt{2}$. The output impedance $Z^E_{\mathrm{out}} = R$ is assumed to be real and constant. The amplifier is considered to be ideal if $\omega_{\mathrm{cut}} = \infty$ and $Z^E_{\mathrm{out}} = 0$ so that $G(\omega) \equiv G^0$ and $H(\omega) \equiv H^0(\omega)$, respectively.

Two bars, one elastic with Young's modulus $E = E^e$ and one viscoelastic with complex modulus

$$E = E^e \frac{t^r}{t^c} \frac{1 + \mathrm{i}\omega t^c}{1 + \mathrm{i}\omega t^r} \tag{33}$$

are considered. Thus, the Young's modulus of the elastic material is the same as the high-frequency limit of the complex modulus which represents the initial elastic response of the viscoelastic material. The parameters t^r and t^c are relaxation and creep time constants, respectively, with $t^r < t^c$ according the three-parameter viscoelastic solid model [15]. As the density ρ of the two bar materials is assumed to be the same, the viscoelastic material approaches the elastic material when the relaxation and creep time constants assume increasingly large values. It is also assumed that the bonding layers are so thin, that their effects on axial stiffness and inertia as well as shear deformation can be neglected.

Eqs. (22), (23), (27) and (32) can be made dimensionless as follows. A reference voltage U_{ref} is taken as a voltage, which characterizes the input voltage U to the amplifier, e.g., the amplitude, and a reference force is defined as $N_{\mathrm{ref}} = 2(A_a E_a d_a/h_a) G^0 U_{\mathrm{ref}}$. This relation is obtained from Eq. (2) by letting $N_a = N_{\mathrm{ref}}/2$, $U_0 = G^0 U_{\mathrm{ref}}$ and $e = 0$. Thus, the reference force is exerted by the two actuators if, with clamped ends, they are driven by the amplifier with the reference voltage as DC input ($|Z^E(0)| = \infty$, $\hat{i}_0(0) = 0$). References for the function H and the gain G (although G is dimensionless) are taken as $H_{\mathrm{ref}} = 2(A_a E_a d_a/h_a)$ and $G_{\mathrm{ref}} = G^0$, respectively, so that there is the relation $N_{\mathrm{ref}} = H_{\mathrm{ref}} G_{\mathrm{ref}} U_{\mathrm{ref}}$ in analogy with Eq. (23). A reference length and a reference time are defined as $x_{\mathrm{ref}} = l_0$ and $t_{\mathrm{ref}} = l_0/c_0^e$, respectively, where $c_0^e = [(2A_a E_a + A_c E^e)/(2A_a \rho_a + A_c \rho)]^{1/2}$ is the common speed of the elastic and viscoelastic wave fronts in the actuator region. Correspondingly, a reference wave propagation coefficient and reference frequencies are defined as $\gamma_{\mathrm{ref}} = 1/x_{\mathrm{ref}}$ and $\omega_{\mathrm{ref}} = f_{\mathrm{ref}} = 1/t_{\mathrm{ref}}$, respectively. Finally, a reference electrical impedance is defined as $Z^E_{\mathrm{ref}} = |Z^E_0(\omega_{\mathrm{ref}})| = 1/2\omega_{\mathrm{ref}} C_a$.

With the dimensionless quantities $\tilde{N} = N/N_{\mathrm{ref}}$, $\hat{\tilde{N}} = \hat{N}/(N_{\mathrm{ref}} t_{\mathrm{ref}})$, … inserted, Eqs. (23) and (32) become

$$\hat{\tilde{N}} = \tilde{H}\tilde{G}\hat{\tilde{U}} e^{-\tilde{\gamma}(\tilde{x}-1/2)}, \tag{34}$$

$$\tilde{G} = \frac{1}{1 + \mathrm{i}\tilde{\omega}/\tilde{\omega}_{\mathrm{cut}}}, \tag{35}$$

respectively. Here, the transfer function $\tilde{H}(\tilde{\omega}) = H(\omega)/H_{\mathrm{ref}} = F(\omega)$ is given by Eqs. (22) with

$$\gamma_0 x_0 = \frac{\mathrm{i}\tilde{\omega}}{2} \left[\left(2\frac{A_a E_a}{A E^e} + \frac{A_c}{A} \right) \Big/ \left(2\frac{A_a E_a}{A E^e} + \frac{A_c}{A} \frac{\tilde{t}^r}{\tilde{t}^c} \frac{1 + \mathrm{i}\tilde{\omega}\tilde{t}^c}{1 + \mathrm{i}\tilde{\omega}\tilde{t}^r} \right) \right]^{1/2}, \tag{36a}$$

$$\frac{Z_0^M}{Z^M} = \left[\left(2\frac{A_a \rho_a}{A\rho} + \frac{A_c}{A} \right) \left(2\frac{A_a E_a}{A E^e} \frac{\tilde{t}^c}{\tilde{t}^r} \frac{1 + \mathrm{i}\tilde{\omega}\tilde{t}^r}{1 + \mathrm{i}\tilde{\omega}\tilde{t}^c} + \frac{A_c}{A} \right) \right]^{1/2}, \tag{36b}$$

$$\frac{Z_a^M}{Z^M} = \frac{1}{\mathrm{i}\tilde{\omega}} \frac{A_a E_a}{A E^e} \left[\frac{\tilde{t}^c}{\tilde{t}^r} \frac{1 + \mathrm{i}\tilde{\omega}\tilde{t}^r}{1 + \mathrm{i}\tilde{\omega}\tilde{t}^c} \left(2\frac{A_a \rho_a}{A\rho} + \frac{A_c}{A} \right) \Big/ \left(2\frac{A_a E_a}{A E^e} + \frac{A_c}{A} \right) \right]^{1/2}, \tag{36c}$$

$$\frac{Z^E_{\mathrm{out}}}{Z^E_0} = \mathrm{i}\tilde{\omega}\tilde{Z}^E_{\mathrm{out}}. \tag{36d}$$

Eq. (27), finally, becomes

$$\tilde{Z}^E = \frac{\tilde{Z}^E_0}{1 - k^2(1 - 4\tilde{F}^0 Z_a^M/Z^M)}, \tag{37}$$

where

$$\tilde{Z}^E_0 = \frac{1}{\mathrm{i}\tilde{\omega}} \tag{38}$$

and $\tilde{F}^0(\tilde{\omega}) = F^0(\omega)$.

The same parameter values $A_aE_a/AE^e = 3$, $A_a\rho_a/A\rho = 1.7$, $A_c/A = 1$ and $k^2 = 0.15$ are chosen for the elastic and viscoelastic bars. For the viscoelastic bar, the relaxation and creep time constants are taken as $\tilde{t}^r = 0.25$ and $\tilde{t}^c = 0.50$, respectively. The cut-off frequency $\tilde{f}_{\text{cut}}$ and the output impedance $\tilde{Z}^E_{\text{out}}$ are varied in the broad intervals $0.01 \leqslant \tilde{f}_{\text{cut}} \leqslant \infty$ and $0 \leqslant \tilde{Z}^E_{\text{out}} \leqslant 10$, respectively. In this way the influence of these parameters can be demonstrated, and the limit case of an ideal amplifier with $\tilde{f}_{\text{cut}} = \infty$ and $\tilde{Z}^E_{\text{out}} = 0$ is included.

4. Results and discussion

Closed-form results have been obtained for the transfer function $H(\omega)G(\omega)$ from the input voltage $\hat{U}(\omega)$ of the amplifier to the output normal force $\hat{N}_0(\omega)$ generated at the actuator/bar interfaces and for the impedance $Z^E(\omega)$ that loads the amplifier. Here, $G(\omega)$ is the voltage gain of the *unloaded* amplifier and $H(\omega)$ is the transfer function from the ideal voltage source $G\hat{U}$ in Fig. 2 to the normal force $\hat{N}_0(\omega)$ generated. This transfer function can also be written as $H_L(\omega)G_L(\omega)$, where

$$G_L = \frac{Z^E}{Z^E + Z^E_{\text{out}}} G, \quad H_L = H^0 \tag{39}$$

are the voltage gain of the *loaded* amplifier and the transfer function from the output voltage of the amplifier to the normal force generated. Here, $H^0(\omega)$ is obtained from $H(\omega)$ by putting $Z^E_{\text{out}} = 0$ in Eqs. (22). Both relations are evident from the equivalent circuit of Fig. 2.

The consistency of the model used has been confirmed by establishing that the mechanical work performed by the actuators on the external parts of the bar is at most equal to the electrical energy supplied to the actuators. This work goes into the energy associated with the waves generated in the bar.

The assumption that initially plane cross-sections remain plane means that the effect of shear deformation of the bonding layers is neglected. In turn, this means that the bonding layers are very thin, or the bonding material is very stiff, or both. Sometimes, it may be consistent to neglect the effects of axial stiffness and inertia together with that of shear deformation, which means that the bonding layers and all their effects are neglected (as in the applications of Section 3). However, the effects of axial stiffness and inertia may be significant even if that of shear deformation is not. If, e.g., the moduli in shear and extension of the bonding layers are increased, the effect of shear deformation decreases while that of axial stiffness increases. At a stage where the shear deformation of the bonding layers can be neglected, the importance of their axial stiffness and inertia is decided by the relative sizes of the middle terms in the expressions $E_0 = (2A_aE_a + 2A_bE_b + A_cE)/A_0$ for the effective complex modulus and $\rho_0 = (2A_a\rho_a + 2A_b\rho_b + A_c\rho)/A_0$ for the effective density.

A necessary condition for the validity of the one-dimensional wave propagation model used is that the significant wavelengths λ associated with the waves generated must be long compared with a characteristic transverse dimension of the bar [16]. If such a dimension is taken as $d = (hw)^{1/2} = A^{1/2}$, this condition can be expressed as $d/\lambda \ll 1$. In the case of the elastic bar, it becomes $1.26(A^{1/2}/l_0)\tilde{f} \ll 1$. If, e.g., $A = 10\,\text{mm}^2$ and $l_0 = 100\,\text{mm}$ one obtains the condition $\tilde{f} \ll 25$. In what follows, numerical results will be presented in the frequency range $0.01 \leqslant \tilde{f} \leqslant 10$.

The frequency dependence of the voltage gain $|\tilde{G}|$ of the unloaded amplifier for different cut-off frequencies $\tilde{f}_{\text{cut}}$ and that of the function $|\tilde{H}|$ for different output impedances $\tilde{Z}^E_{\text{out}}$ are shown in Figs. 3(a) and (b) for the elastic bar and in Figs. 4(a) and (b) for the viscoelastic bar. The frequency dependence of the impedance $\tilde{Z}^E$ that loads the amplifier is shown in Figs. 3(c) for the elastic bar and in Fig. 4(c) for the viscoelastic bar.

In the elastic case, anti-resonance occurs at the frequencies $\tilde{f}_n = n$, $n = 1, 2, 3, \ldots$, which are the zeroes of $\tilde{H}(2\pi\tilde{f})$ in addition to the zero at $\tilde{f} = 0$. These frequencies correspond to periods that are 1, 1/2, 1/3, … transit times $t = 0$ through the actuator region and wavelengths that are 1, 1/2, 1/3, … of the length l_0 of this region. At these frequencies, both the normal forces $\hat{\tilde{N}}_0$ and the particle velocities $\pm\hat{\tilde{v}}_0$ at the actuator/bar interfaces are zero. This implies that no work is performed at these interfaces and no waves are generated in the external parts of the bar. Therefore, there are no external losses associated with the vibrations in the actuator region. In addition, there are no internal losses as the materials of the actuator region are elastic. This total absence of losses explains the perfect sharpness and depth to zero of the minima of $|\tilde{H}|$ at the anti-resonance frequencies.

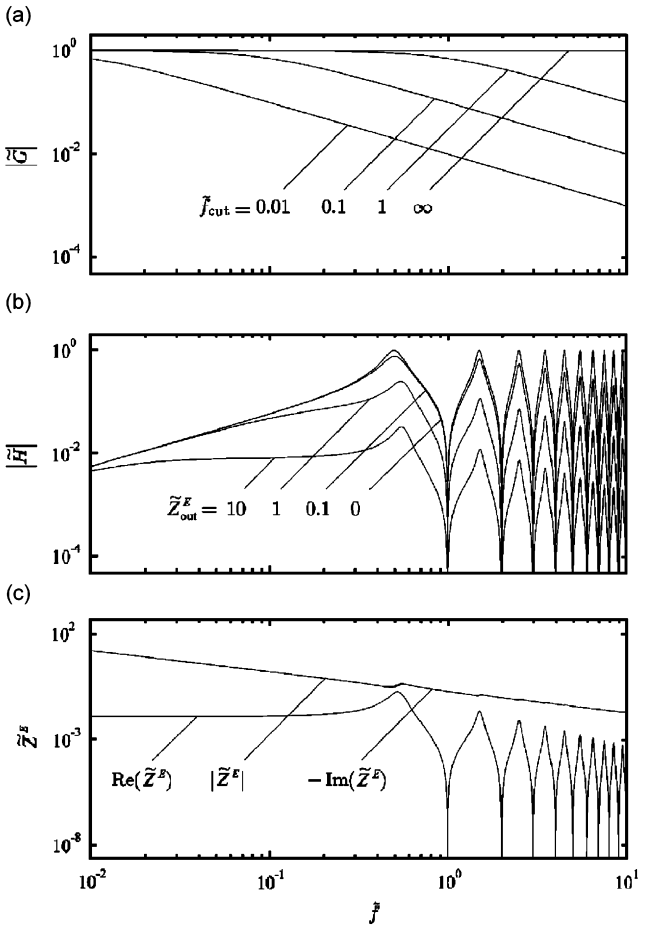

Fig. 3. Dependence on frequency $\tilde{f}$ of (a) the voltage gain $|\tilde{G}|$ for different cut-off frequencies $\tilde{f}_{\mathrm{cut}}$, (b) the function $|\tilde{H}|$ for different output impedances $\tilde{Z}^E_{\mathrm{out}}$, and (c) the load impedance $\tilde{Z}^E$. Elastic bar.

Between these frequencies, the function $|\tilde{H}|$ has local maxima. The maximum values are $|\tilde{H}|_{\max} \approx 1$ for an ideal amplifier with $\tilde{Z}^E_{\mathrm{out}} = 0$, and they decrease with increasing output impedance $\tilde{Z}^E_{\mathrm{out}}$. This decrease is larger at higher than at lower frequencies.

It may seem abnormal that the actuator region can vibrate in modes such that both the normal force and the particle velocity are zero at its ends. However, Eqs. (17)–(20) and (22a) show how this is possible. The last of these equations show that at the anti-resonance frequencies $\mathrm{e}^{-\gamma_0 x_0} = \mathrm{e}^{\gamma_0 x_0}$. Substitution into Eq. (18) shows that $\hat{v}_0 = 0$. This result, the conditions of continuity and Eqs. (19) and (20) show that also $\hat{N}_0 = 0$. Eq. (17), with $x = x_0$ and $\hat{N} = \hat{N}_0 = 0$, shows how the amplitudes $\hat{N}_{0p}(\omega) = \hat{N}_{0n}(\omega)$ of the waves $\hat{N}_{0p}e^{-\gamma_0 x}$ and $\hat{N}_{0n}e^{\gamma_0 x}$ within the actuator region depend on the input voltage $\hat{U}$ of the amplifier. Conversely, this equation shows that vibrations with both $\hat{N}_0 = 0$ and $\hat{v}_0 = 0$ would not be possible if either $\hat{U} = 0$ (natural vibrations) or $d_a = 0$ (non-piezoelectric material).

Figs. 3 and 4(c) show that the load impedance $\tilde{Z}^E$ has a relatively small real part which is non-negative, $0 \leqslant \mathrm{Re}(\tilde{Z}^E) \ll |\tilde{Z}^E|$, and a relatively large imaginary part which is negative, $0 < -\mathrm{Im}(\tilde{Z}^E) \approx |\tilde{Z}^E|$. For maximum supply of power to the actuators, the load impedance should be the complex conjugate of the output impedance of the amplifier [17], i.e., $\tilde{Z}^E = \bar{\tilde{Z}}^E_{\mathrm{out}}$. As the output impedance has been taken as real, $\tilde{Z}^E_{\mathrm{out}} = \tilde{R}$, this condition implies $\mathrm{Re}(\tilde{Z}^E) = \tilde{R}$ and $\mathrm{Im}(\tilde{Z}^E) = 0$. The first of these matching conditions can be satisfied at one or several discrete frequencies provided that $\tilde{R} \leqslant 0.18$. It can also be satisfied in an approximate

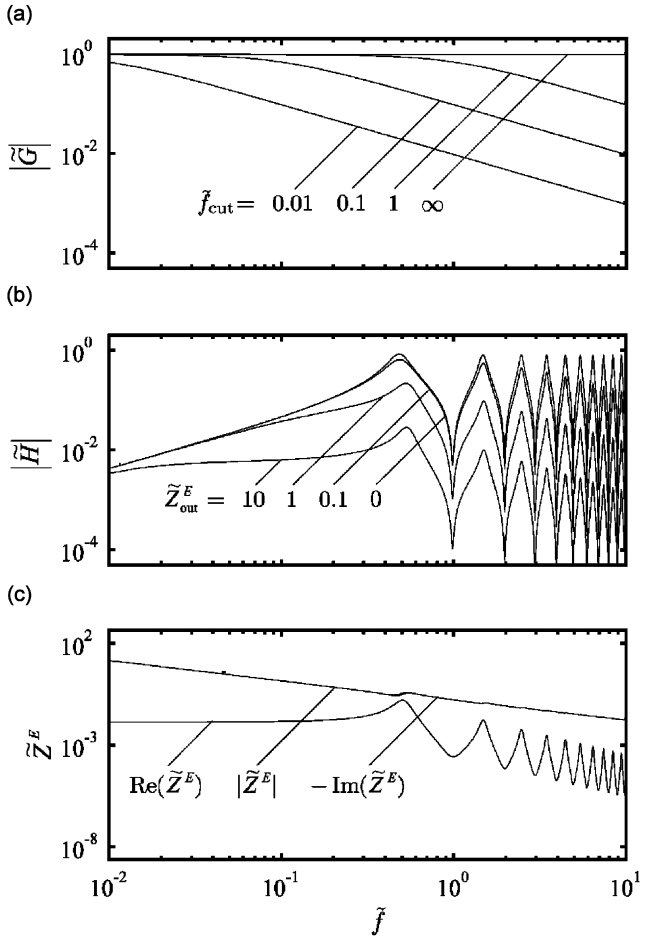

Fig. 4. Dependence on frequency $\tilde{f}$ of (a) the voltage gain $|\tilde{G}|$ for different cut-off frequencies $\tilde{f}_{\mathrm{cut}}$, (b) the function $|\tilde{H}|$ for different output impedances $\tilde{Z}^E_{\mathrm{out}}$, and (c) the load impedance $\tilde{Z}^E$. Viscoelastic bar.

sense within a limited range of frequencies. The second condition can be satisfied at a chosen frequency by means of a matching inductance which is included in the load. It can also be satisfied in an approximate sense within a limited range of frequencies.

In the elastic case, $\mathrm{Re}(\tilde{Z}^E)$ has zeroes at the anti-resonance frequencies $\tilde{f}_n = n$, $n = 0, 1, 2, \ldots$, which are the zeroes of $\tilde{H}(2\pi\tilde{f})$ and $\tilde{H}^0(2\pi\tilde{f})$. Eqs. (37) and (38) show that at these frequencies, the load impedance is imaginary, $\tilde{Z}^E = 1/\mathrm{i}\tilde{\omega}(1-k^2)$. Consequently, the average power supplied by the amplifier to the actuators is zero. This is consistent with the observation that no work is performed on the external parts of the bars at the anti-resonance frequencies and with the absence of internal losses. Between the anti-resonance frequencies, the real part $\mathrm{Re}(\tilde{Z}^E)$ has local maxima, similarly as $|\tilde{H}|$, and the maximum values decrease with increasing frequency.

In the cases considered, with $0 \leqslant \mathrm{Re}(\tilde{Z}^E) \ll |\tilde{Z}^E|$ and $0 < -\mathrm{Im}(\tilde{Z}^E) \approx |\tilde{Z}^E|$, the load impedance at the anti-resonance frequencies can be used to approximate the imaginary part of the load impedance at all frequencies, i.e., $\mathrm{Im}(\tilde{Z}^E) \approx -1/\tilde{\omega}(1-k^2)$. In dimensional terms $\mathrm{Im}(Z^E) \approx -1/\omega 2(1-k^2)C_a$, which shows that the imaginary part of the load can be represented by a capacitance $C \approx 2(1-k^2)C_a$. This capacitance can be regarded as the capacitance $2C_a$ in series with a capacitance $2C_a(1-k^2)/k^2$, which is $\gg 2C_a$ if $k^2 \ll 1$.

In the viscoelastic case, the behaviour of the load impedance $\tilde{Z}^E(\omega)$ between antiresonance frequencies is similar to that in the elastic case. However, the minima in $\mathrm{Re}(\tilde{Z}^E)$ are less sharp and deep in the viscoelastic case than in the elastic case. This is in accord with the behaviour of $|\tilde{H}|$.

The responses of the normal force $\tilde{N}_0(\tilde{t})$ at the actuator/bar interfaces, for different combinations of the cut-off frequency $\tilde{f}_{\text{cut}}$ and the output impedance $\tilde{Z}^E_{\text{out}}$, to a unit step input voltage $\tilde{U}(\tilde{t}) = \theta(\tilde{t})$ to the amplifier are shown in Fig. 5 for the elastic bar and in Fig. 6 for the viscoelastic bar. In both cases, the responses have damped oscillatory behaviour due to the repeated reflections of waves between the actuator/bar interfaces. For infinite cut-off frequency and zero output impedance, the zeroes of $\tilde{N}_0(\tilde{t})$ occur at $\tilde{t} = 0, 1, 2, \ldots$, i.e., at distances from each other equal to the transit time t_0 for an elastic or viscoelastic wave front through the actuator region. These distances increase and the maximum amplitude decreases with decreasing cut-off frequency and increasing output impedance. This is because an increase of output impedance, similarly as a decrease of cut-off frequency, increases the slowness of the response of the loaded amplifier. In the applications considered, a characteristic response time of the loaded amplifier may be taken as the product $t_{RC} = RC$ of the assumed resistive output impedance R of the amplifier and the approximate input capacitance $C \approx 2(1-k^2)C_a$ of the actuators, which gives $\tilde{t}_{RC} = (1-k^2)\tilde{Z}^E_{\text{out}}$. Thus, in dimensionless terms, this response time is directly proportional to the assumed resistive output impedance. It represents the time needed to charge the capacitance C from zero to 63% of full DC voltage through the resistance R.

Conversely, the input voltages $\tilde{U}(\tilde{t})$ required to produce the normal force pulse $\tilde{N}_0(\tilde{t}) = [\theta(\tilde{t}) - \theta(\tilde{t}-\tilde{T})]\sin(2\pi\tilde{t}/\tilde{T})$ with duration $\tilde{T} = 50$, for amplifiers with cut-off frequency $\tilde{f}_{\text{cut}} = 1$ and the output impedances $\tilde{Z}^E_{\text{out}} = 0$ and 10, are shown in Fig. 7 for the elastic bar and in Fig. 8 for the viscoelastic bar. The input voltage amplitude required increases with increasing output impedance, and it is higher for the viscoelastic bar than for the stiffer elastic bar.

The spectrum $|\hat{\tilde{N}}_0(2\pi\tilde{f})|$ is shown in Fig. 9, where it can be seen that frequencies $\tilde{f} > 0.5$ are not significant. Furthermore, Figs. 3 and 4 show that the function $\tilde{H}^{-1}\tilde{G}^{-1}$ is well-behaved for non-zero frequencies, which are well below the lowest anti-resonance frequency $f_1 = 1$. Therefore, the maximum frequency for the DFT inversion was taken as $\tilde{f}_{\max} = \frac{1}{2}$, which resulted in a sufficiently accurate discrete representation of $\tilde{N}_0(\tilde{t})$. If the desired pulse would have a considerably broader spectrum, in particular with significant frequencies $\tilde{f} > 1$, numerical problems are likely and it may not be possible to determine the required input $\tilde{U}(\tilde{t})$.

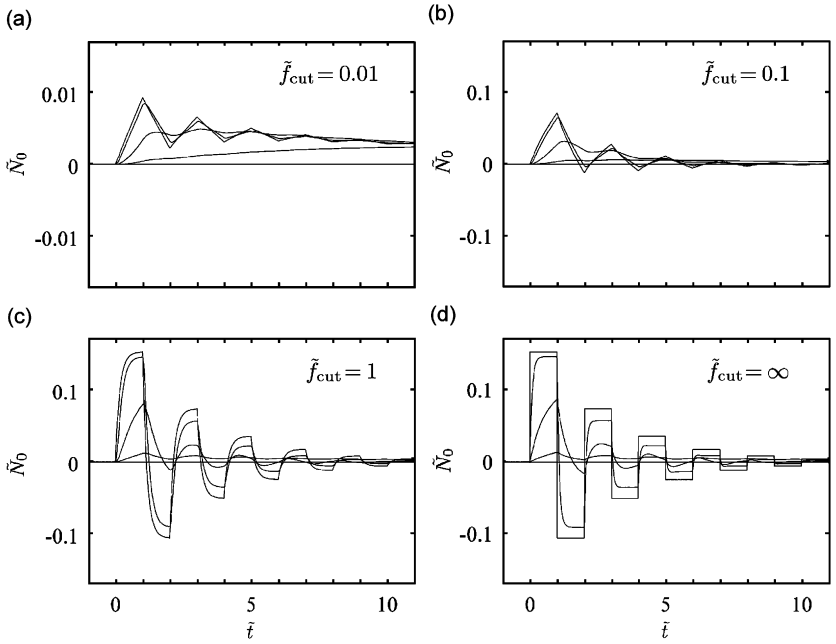

Fig. 5. Normal force $\tilde{N}_0$ versus time $\tilde{t}$ at actuator/bar interfaces in response to a unit step amplifier input voltage for different cut-off frequencies: (a) $\tilde{f}_{\text{cut}} = 0.01$, (b) $\tilde{f}_{\text{cut}} = 0.1$, (c) $\tilde{f}_{\text{cut}} = 1$ and (d) $\tilde{f}_{\text{cut}} = \infty$. The amplitude in each diagram decreases with increasing output impedance $\tilde{Z}^E_{\text{out}} = 0$, 0.1, 1 and 10. Elastic bar.

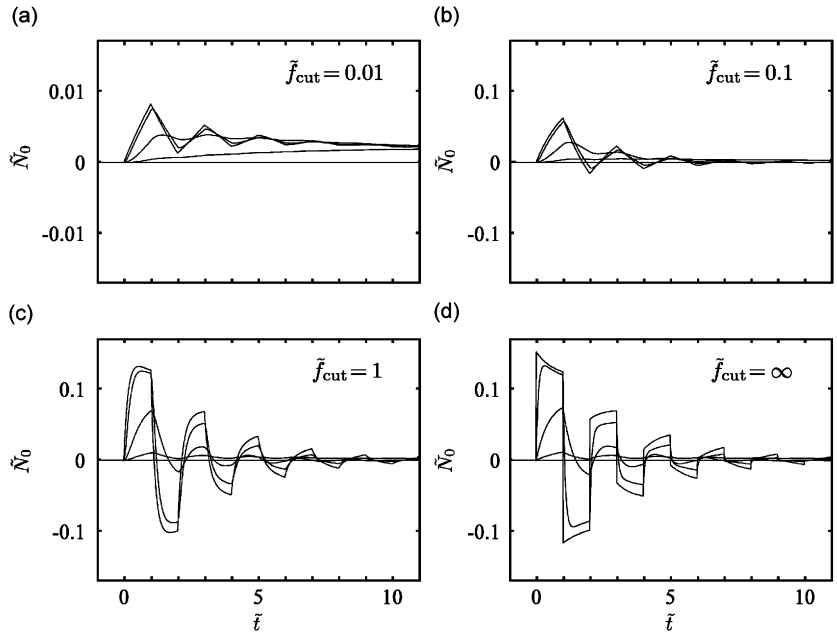

Fig. 6. Normal force $\tilde{N}_0$ versus time $\tilde{t}$ at actuator/bar interfaces in response to a unit step amplifier input voltage for different cut-off frequencies: (a) $\tilde{f}_{\mathrm{cut}}=0.01$, (b) $\tilde{f}_{\mathrm{cut}}=0.1$, (c) $\tilde{f}_{\mathrm{cut}}=1$ and (d) $\tilde{f}_{\mathrm{cut}}=\infty$. The amplitude in each diagram decreases with increasing output impedance $\tilde{Z}^{E}_{\mathrm{out}}=0$, 0.1, 1 and 10. Viscoelastic bar.

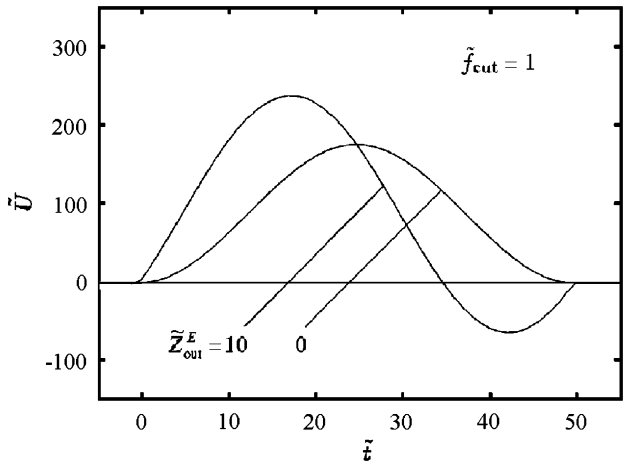

Fig. 7. Amplifier input voltage $\tilde{U}$ versus time $\tilde{t}$ required to generate a single-period sine normal force with unit amplitude and duration 50 at actuator/bar interfaces. Cut-off frequency $\tilde{f}_{\mathrm{cut}}=1$. Amplitude increasing with increasing output impedance $\tilde{Z}^{E}_{\mathrm{out}}=0$ and 10. Elastic bar.

5. Conclusions

The main conclusions of this study are as follows: (i) In the case of an elastic bar, anti-resonance occurs at frequencies that are integer multiples of the inverse transit time through the actuator region. At these frequencies, the actuator region vibrates without internal or external losses, and therefore the anti-resonance minima have perfect sharpness and depth to zero. (ii) In the case of a viscoelastic bar, the behaviour between the anti-resonance frequencies is similar as in that of an elastic bar, but the minima are less sharp and deep due to internal as well as external losses. (iii) The impedance of the actuators, which constitutes the load of the

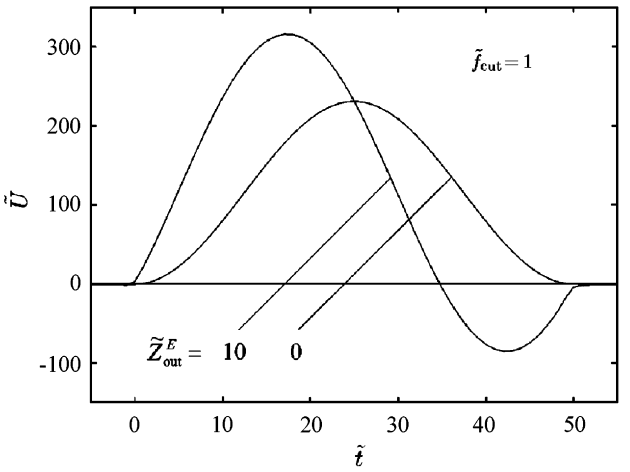

Fig. 8. Amplifier input voltage $\tilde{U}$ versus time $\tilde{t}$ required to generate a single-period sine normal force with unit amplitude and duration 50 at actuator/bar interfaces. Cut-off frequency $\tilde{f}_{cut}=1$. Amplitude increasing with increasing output impedance $\tilde{Z}^E_{out}=0$ and 10. Viscoelastic bar.

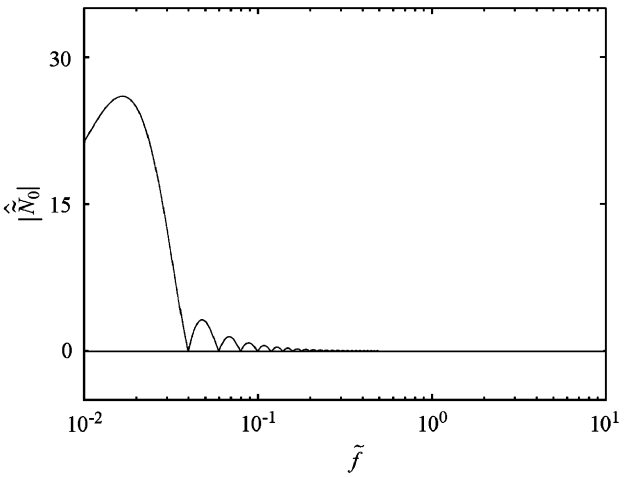

Fig. 9. Spectrum $|\hat{\tilde{N}}_0|$ versus frequency $\tilde{f}$ of single-period sine normal force with unit amplitude and duration 50.

amplifier, has a relatively small non-negative real part and a relatively large negative imaginary part. (iv) Perfect matching of the actuator load impedance to the output impedance of the amplifier can be achieved only at discrete frequencies and with the aid of a matching inductance. Within a limited range of frequencies, approximate matching can be achieved similarly. (v) In the case of an elastic bar, the real part of the load impedance has its zeroes at the anti-resonance frequencies. In an approximate sense, the imaginary part can be represented by a capacitance at all frequencies. (vi) In the case of a viscoelastic bar, the behaviour of the load impedance between the anti-resonance frequencies is similar as in that of an elastic bar, but the minima of the real part are less sharp and deep. (vii) The normal force at the actuator/bar interfaces in response to a step input voltage to the amplifier has a damped oscillatory behaviour due to repeated reflections of waves between the actuator/bar interfaces. (viii) An increase of output impedance increases the slowness of the response of the loaded amplifier due to the capacitive nature of the amplifier load. A decrease of cut-off frequency increases the slowness of the response of the loaded amplifier similarly. (ix) The input voltage to the amplifier required to produce a desired normal force pulse at the actuator/bar interfaces can be determined provided that the spectrum of this pulse is not too broad.

Acknowledgements

The authors gratefully acknowledge economical support from the Swedish Research Council (Contract no. 621-2001-2156).

References

[1] G. Gautschi, *Piezoelectric Sensorics*, Springer, Berlin, Heidelberg, 2002.
[2] R. Puers, W. Claes, W. Sansen, M. De Cooman, J. Duyck, I. Naert, Towards the limits in detecting low-level strain with multiple piezo-resistive sensors, *Sensors and Actuators A (Physical)* 85 (2000) 395–401.
[3] J.K. Dürr, R. Honke, M. von Alberti, R. Sippel, Development of an adaptive lightweight mirror for space application, *Smart Materials and Structures* 12 (2003) 1005–1016.
[4] K.K. Tan, S.C. Ng, S.N. Huang, Assisted reproduction system using piezo actuator. *2004 International Conference on Communications, Circuits and Systems* (*IEEE Cat. No. 04EX914*), 2004, Vol. 2(part 2), p. 1200-3.
[5] T. Ikeda, *Fundamentals of Piezoelectricity*, Oxford University Press, New York, 1990.
[6] E.F. Crawley, J. de Luis, Use of piezoelectric actuators as elements of intelligent structures, *AIAA Journal* 25 (10) (1987) 1373–1385.
[7] J. Pan, C.H. Hansen, S.D. Snyder, A study of the response of a simply supported beam to excitation by a piezoelectric actuator, *Journal of Intelligent Material Systems and Structures* 3 (1) (1992) 3–16.
[8] N.W. Hagood, W.H. Chung, A. von Flotow, Modelling of piezoelectric actuator dynamics for active structural control, *Journal of Intelligent Material Systems and Structures* 1 (3) (1990) 327–354.
[9] R.P. Thornburgh, A. Chattopadhyay, Simultaneous modeling of mechanical and electrical response of smart composite structures, *AIAA Journal* 40 (8) (2002) 1603–1610.
[10] R.P. Thornburgh, A. Chattopadhyay, A. Ghoshal, Transient vibration of smart structures using a coupled piezoelectric-mechanical theory, *Journal of Sound and Vibration* 274 (2004) 53–72.
[11] N.W. Hagood, A. von Flotow, Damping of structural vibrations with piezoelectric materials and passive electrical networks, *Journal of Sound and Vibration* 146 (1991) 243–268.
[12] C. Niezrecki, H.H. Cudney, Improving the power consumption characteristics of piezoelectric actuators, *Journal of Intelligent Material Systems and Structures* 5 (1994) 522–529.
[13] D.J. Leo, Energy analysis of piezoelectric-actuated structures driven by linear amplifiers, *Journal of Intelligent Material Systems and Structures* 10 (1) (1999) 36–45.
[14] R.M. Christensen, Restrictions upon viscoelastic relaxation functions and complex moduli, *Transactions of The Society of Rheology* 16 (4) (1972) 603–614.
[15] W. Flügge, *Viscoelasticity*, Springer, Berlin, Heidelberg, 1975.
[16] H. Kolsky, *Stress Waves in Solids*, Dover Publications, Inc., New York, 1963.
[17] P. Lorrain, D.R. Corson, *Electromagnetism: Principles and Applications*, second ed., W.H. Freeman and Company, New York, 1997.